Ultraslow optical solitons in atomic media with spontaneously generated coherence

Chao Hang* and Guoxiang Huang

State Key Laboratory of Precision Spectroscopy and Department of Physics, East China Normal University, Shanghai 200062, China
**Corresponding author: chang@phy.ecnu.edu.cn*

Received March 19, 2012; revised May 9, 2012; accepted June 6, 2012;
posted June 8, 2012 (Doc. ID 165019); published July 17, 2012

We propose a new scheme to generate stable ultraslow optical solitons in lifetime-broadened three-state V-type media via spontaneously generated coherence (SGC). We show that in the linear propagation regime, SGC in the system can result in a significant change of dispersion and absorption, which may be used to completely eliminate absorption and greatly reduce the group velocity of the probe field. In the nonlinear propagation regime, SGC can largely enhance the Kerr nonlinearity of the system. By means of SGC, stable optical solitons with ultraslow propagating velocity and ultralow generation power can be produced. Different from previous works, ultraslow optical solitons obtained in the present system based on SGC have much smaller attenuation during propagation and can be created by using only one laser field.

OCIS codes: 190.5530, 030.1640.

1. INTRODUCTION

The propagation of nonlinear optical pulses in resonant atomic media has been an important subject of many studies. A lot of progress has been made in this research direction, including the solitons via the self-induced transparency [1] and the simultons and adiabatons in multilevel media [2,3]. The formation of such nonlinear localized structures is obtained only for short, strong nonlinear optical pulses, with the propagating velocity not far from the light speed in vacuum.

Recently, much attention has been paid to optical pulse propagation in coherent resonant media via electromagnetic-induced transparency (EIT) [4]. Because of the quantum interference effect induced by a coupling laser field, the absorption of a probe laser field propagating in an EIT medium can be largely eliminated. In addition, a drastic change of dispersion of the system occurs, which results in a significant reduction of group velocity of the probe field. The drastic change of dispersion, however, inevitably leads to a serious distortion of the probe field during propagation. In order to suppress such distortion, a weak nonlinear effect of the system has been used to balance the dispersion, which leads to a new class of optical solitons, i.e., ultraslow optical solitons [5–7], achievable at a very low light level. Such shape-preserving slow light pulses with low light intensity have potential applications in optical and quantum information processing and transmission and deserve to be pursued in the fields of fundamental research and technological development.

However, in EIT media it is crucial to have at least two laser fields to create an atomic coherence. In addition, although the linear optical absorption can be largely eliminated by the coupling field, it cannot be eliminated completely. The existence of the absorption results in attenuation of the probe field during propagation. Especially, the attenuation will be significant when propagation distance is long. Note that besides the EIT technique, another type of important atomic coherence can also be created by exploiting the quantum interference between two spontaneous emission channels without using any coupling laser field, which is called spontaneously generated coherence (SGC). SGC was first discovered in the context of V-type media by Agarwal [8]. In recent years, much attention has been paid to the study of SGC and related topics, including lasing without inversion [9–12], coherent population trapping [13], spectral narrowing and fluorescence quenching [14–18], fluorescence squeezing [19], giant self-phase modulation [20], ground-state quantum beats [21], cavity-mode entanglement [22], electromagnetically induced gratings [23], and so on.

Although a large amount of research activities has been done on SGC, most of it is focused on static properties, and only a few works are dedicated to the study of pulse propagation in SGC media. Here we mention the work by Paspalakis *et al.* [24] who studied pulse propagation in a four-level system, where the ground state is coupled to two closely spaced excited states by only a laser field. In that work, the optical fields involved are intense enough so that the optical absorption and pulse distortion can be neglected. Optical pulse propagation with an adiabatonlike property is observed by using numerical simulations.

In this article, we investigate, both analytical and numerically, the stable ultraslow optical solitons in lifetime-broadened three-state V-type media with SGC. Instead of adiabatons, we consider breatherlike weak nonlinear excitations without using any adiabatic approximation. Our work includes two aspects: (i) we study the linear propagating properties of the probe field with the SGC effect being taken into account. We show that SGC in such a system can result in a significant change of dispersion and absorption. In particular, SGC can completely eliminate the linear absorption of the probe field. At the same time, the group velocity of the probe field is largely reduced. (ii) We demonstrate that in the nonlinear propagation regime, SGC can largely enhance the Kerr nonlinearity of the system. By using SGC, stable optical

solitons with ultraslow propagating velocity and ultralow generation power can be produced. We stress that the scheme for generating ultraslow optical solitons presented in this work is very different from those obtained based on EIT [5–7] because the linear absorption of the system is completely suppressed and only one laser field is needed in the soliton-generating process. To the best of our knowledge, this is the first study on optical solitons in resonant atomic media with SGC.

The rest of the article is arranged as follows. In Section 2, the model of three-state V-type configurations with SGC is introduced. Linear pulse propagations are discussed, and dispersion and absorption properties are analyzed. In Section 3, the Kerr nonlinearity of the system is analyzed and ultraslow optical solitons at very low light level are obtained. Finally, Section 4 contains a summary of our main results.

2. MODELS AND PULSE PROPAGATION IN THE LINEAR REGIME

We consider a three-level V-type atomic system, as shown in Fig. 1(a), in which two closely spaced excited states $|2\rangle$ and $|3\rangle$ decay simultaneously into the ground state $|1\rangle$ by the spontaneous emission with decay rates Γ_2 and Γ_3, respectively. The quantum interference between the two decay channels (from $|2\rangle$ to $|1\rangle$ and $|3\rangle$ to $|1\rangle$) results in SGC of the system [25]. A weak, pulsed probe field (with duration τ_0) of center frequency ω_p and wave vector $\mathbf{k}_p$, i.e., $\mathbf{E}_p(\mathbf{r},t)=\mathbf{e}_p\mathcal{E}_p(\mathbf{r},t)e^{i(\mathbf{k}_p\cdot\mathbf{r}-\omega_p t)}+\text{c.c}$, couples the ground state $|1\rangle$ to the excited states $|2\rangle$ and $|3\rangle$, where $\mathbf{e}_p$ and $\mathcal{E}_p(\mathbf{r},t)$ are the unit polarization vector and envelope function of the probe field, respectively.

Under electric-dipole, rotating-wave, and Weisskopf–Wigner approximations, the equations of motion for the density matrix governing atomic dynamics are

$$\dot{\rho}_{22}=-\Gamma_2\rho_{22}+i\Omega_p\rho_{12}-i\Omega_p^*\rho_{21}-\eta\frac{\sqrt{\Gamma_2\Gamma_3}}{2}(\rho_{23}+\rho_{32}), \quad (1)$$

$$\dot{\rho}_{33}=-\Gamma_3\rho_{33}+ip\Omega_p\rho_{13}-ip\Omega_p^*\rho_{31}-\eta\frac{\sqrt{\Gamma_2\Gamma_3}}{2}(\rho_{23}+\rho_{32}), \quad (2)$$

$$\dot{\rho}_{21}=\left[i(\Delta+\delta)-\frac{\Gamma_2}{2}\right]\rho_{21}+i\Omega_p(\rho_{11}-\rho_{22})-ip\Omega_p\rho_{23}-\eta\frac{\sqrt{\Gamma_2\Gamma_3}}{2}\rho_{31}, \quad (3)$$

$$\dot{\rho}_{31}=\left[i(-\Delta+\delta)-\frac{\Gamma_3}{2}\right]\rho_{31}+ip\Omega_p(\rho_{11}-\rho_{33})-i\Omega_p\rho_{32}-\eta\frac{\sqrt{\Gamma_2\Gamma_3}}{2}\rho_{21}, \quad (4)$$

$$\dot{\rho}_{32}=-\left(i2\Delta+\frac{\Gamma_2+\Gamma_3}{2}\right)\rho_{32}-i\Omega_p^*\rho_{31}+ip\Omega_p\rho_{12}-\eta\frac{\sqrt{\Gamma_2\Gamma_3}}{2}(\rho_{22}+\rho_{33}), \quad (5)$$

with $\rho_{11}+\rho_{22}+\rho_{33}=1$. Here $\Omega_p=\mathbf{e}_p\cdot\mathbf{d}_{12}\mathcal{E}_p/\hbar$ is half the Rabi frequency of the probe field, with $\mathbf{d}_{ij}\equiv\langle i|\mathbf{d}|j\rangle$ being the density-matrix elements related to states $|i\rangle$ and $|j\rangle$, $\Delta=(E_3-E_2)/(2\hbar)$ is the half-frequency difference between $|2\rangle$ and $|3\rangle$, and $\delta=\omega_p-(E_3+E_2)/(2\hbar)$ is one-photon detuning [see Fig. 1(a)]. The cross-coupling term contributed by the SGC effect is manifested by the factor $\eta\sqrt{\Gamma_2\Gamma_3}/2$, with $\eta=\mathbf{d}_{12}\cdot\mathbf{d}_{13}/|\mathbf{d}_{12}||\mathbf{d}_{13}|=\cos\theta$ denoting the alignment of two dipole matrix elements $\mathbf{d}_{12}$ and $\mathbf{d}_{13}$, where θ is the misalignment angle between $\mathbf{d}_{12}$ and $\mathbf{d}_{13}$ [see Fig. 1(b)]. If $\mathbf{d}_{12}$ and $\mathbf{d}_{13}$ are parallel (i.e., $\theta=0$), one has $\eta=1$, the system exhibits maximum SGC; if $\mathbf{d}_{12}$ and $\mathbf{d}_{13}$ are perpendicular (i.e., $\theta=\pi/2$), one has $\eta=0$, the system displays no SGC. $p=|\mathbf{e}_p\cdot\mathbf{d}_{13}|/|\mathbf{e}_p\cdot\mathbf{d}_{12}|=|\mathbf{d}_{13}|\cos\theta_1/[|\mathbf{d}_{12}|\cos\theta_2]$, where θ_1 (θ_2) is the misalignment angle between $\mathbf{d}_{12}$ ($\mathbf{d}_{13}$) and $\mathbf{e}_p$. In the following, we assume $|\mathbf{d}_{13}|\simeq|\mathbf{d}_{12}|$ and a particular case can be found that θ is equally partitioned by $\mathbf{e}_p$, i.e., $\theta_1\simeq\theta_2=\theta/2$, as in [23]. In such a case, we have $p\simeq1$ and $-1\le\eta\le1$.

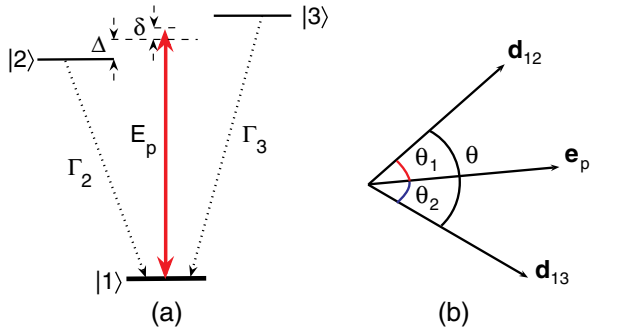

Fig. 1. (Color online) Energy level diagrams and excitation schemes of lifetime-broadened V-type three-level systems with SGC. Here, $|j\rangle$ ($j=1,2,3$) are atomic bare states, $\mathbf{E}_p$ is a weak probe laser field, Δ and δ are detunings, and Γ_j ($j=1,2$) are decay rates of relevant states. (b) The definition of the alignment angles (θ_1, θ_2) of the dipole matrix elements ($\mathbf{d}_{12}$, $\mathbf{d}_{13}$) related to the unit polarization vector $\mathbf{e}_p$ of the probe field. $\theta=\theta_1+\theta_2$ is the angle between $\mathbf{d}_{12}$ and $\mathbf{d}_{13}$.

The equation of motion for the probe-field Rabi frequency Ω_p can be obtained by using the Maxwell equation. Under slowly varying envelope approximation, it reads

$$i\left(\frac{\partial}{\partial z}+\frac{1}{c}\frac{\partial}{\partial t}\right)\Omega_p+\kappa(\rho_{21}+p\rho_{31})=0, \quad (6)$$

where $\kappa=\mathcal{N}_a\omega_p|\mathbf{e}_p\cdot\mathbf{d}_{12}|^2/(2\epsilon_0c\hbar)$ with $\mathcal{N}_a$ being the atomic concentration. For simplicity, we assume in the following that $\Gamma_2\approx\Gamma_3\equiv\Gamma$.

The linear optical response of the system can be obtained by solving the Maxwell–Bloch Eqs. (1) and (6). Assuming Ω_p is a small quantity, $\rho_{11}\approx1$, and ρ_{21}, ρ_{31}, and Ω_p are proportional to $\exp[i(Kz-\omega t)]$, we obtain the linear dispersion relation

$$K(\omega)=\frac{\omega}{c}-\kappa\left[\frac{\omega+d_3-ip\eta\Gamma/2}{D(\omega)}+\frac{p^2(\omega+d_2)-ip\eta\Gamma/2}{D(\omega)}\right], \quad (7)$$

where $D(\omega)=(\omega+d_2)(\omega+d_3)+\eta^2\Gamma^2/4$ with $d_2=\Delta+\delta+i\Gamma/2$, and $d_3=-\Delta+\delta+i\Gamma/2$. By Taylor expanding $K(\omega)$ around $\omega=0$ [26], we obtain $K(\omega)=K_0+K_1\omega+\frac{1}{2}K_2\omega^2+\cdots$, with the expansion coefficients $K_j=[\partial^jK(\omega)/\partial\omega^j]|_{\omega=0}$ ($j=0,1,2,\cdots$) explicitly given by $K_0=-\kappa(p^2d_2+d_3-ip\eta\Gamma)/(d_2d_3+\eta^2\Gamma^2/4)$, $K_1=1/c-\kappa(1+p^2)/(d_2d_3+\eta^2\Gamma^2/4)+\kappa(p^2d_2+d_3-ip\eta\Gamma)(d_2+d_3)/(d_2d_3+\eta^2\Gamma^2/4)^2$, and $K_2=2\kappa(1+p^2)(d_2+d_3)/(d_2d_3+\eta^2\Gamma^2/4)^2+2\kappa(p^2d_2+d_3-ip\eta\Gamma)/(d_2d_3+\eta^2\Gamma^2/4)^2-2\kappa(p^2d_2+d_3-ip\eta\Gamma)(d_2+d_3)^2/(d_2d_3+\eta^2\Gamma^2/4)^3$. Here, $K_0=\text{Re}(K_0)+i\text{Im}(K_0)$ gives the phase shift

per unit length and absorption coefficient, K_1 determines the group velocity $V_g(\equiv 1/\mathrm{Re}K_1)$, and K_2 represents the group-velocity dispersion.

Shown in Figs. 2(a) and 2(b) are, respectively, the real and imaginary parts of K as functions of ω, which characterize the dispersion and absorption of the system. The solid lines in the figure are for the case with the maximum SGC (i.e., $\eta = 1$), whereas the dashed lines are for the case without SGC (i.e., $\eta = 0$). System parameters are chosen as $\kappa = 1.0 \times 10^9$ cm^{-1} s^{-1}, $\Gamma = 1.0 \times 10^7$ s^{-1}, $\Delta = 1.0 \times 10^7$ s^{-1}, $\delta = 0$, and $p = 1$. We see that in the region around $\omega = 0$ the probe-field displays a drastic change of dispersion [and hence a drastic reduction of group velocity—panel (a)] and a large suppression of absorption [panel (b)]. Obviously, the reduction of group velocity and the suppression of absorption with SGC are much more significant than those without SGC.

It is instructive to discuss the SGC effect on the probe-field absorption in more detail. From Fig. 2(b), we see that the probe-field absorption is suppressed around $\omega = 0$ in cases with and without SGC, resulting in the appearance of transparency windows in the absorption spectrum. However, the depth and width of the transparency windows are quite different. The transparency window with the maximum SGC ($\eta = 1$, the solid curve) is much more deeper and wider than that without SGC ($\eta = 0$, the dashed curve).

The difference for the absorption spectra for the above two cases can be understood more clearly by using the "decaying-dressed states" [27,28]. For this aim, we can express $K(\omega)$ into the form

$$K(\omega) = \frac{\omega}{c} + R_1 + R_2, \tag{8}$$

where

$$R_1 = -\kappa \frac{K_+}{\omega - \omega_+}, \qquad R_2 = -\kappa \frac{K_-}{\omega - \omega_-}, \tag{9}$$

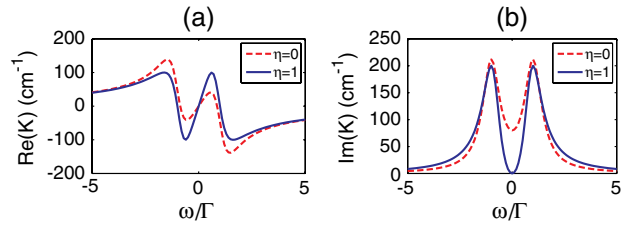

Fig. 2. (Color online) (a) Re(K) and (b) Im(K) as functions of ω/Γ with maximum SGC (i.e., $\eta = 1$, the solid curve) and without SGC (i.e., $\eta = 0$, the dashed curve).

denote two resonances with poles $\omega_\pm = -(\delta + i\Gamma/2) \pm \sqrt{\Delta^2 - \eta^2\Gamma^2/4}$ and amplitudes $K_\pm = \pm[(1+p^2)\omega_\pm + p^2 d_2 + d_3 - ip\eta\Gamma]/\sqrt{4\Delta^2 - \eta^2\Gamma^2}$, respectively.

Each panel in Fig. 3 displays the imaginary part of the two resonances separately [Im(R_1) and Im(R_2), the solid and dashed curves] and their combination as the total absorption [Im(K); the dotted curve]. The system parameters are the same with those used in Fig. 2. In the left panels we show the spectra without SGC ($\eta = 0$) with the increasing value of Δ/Γ. A dip with nonzero minimum in the total absorption can be interpreted as a gap between the two resonances, which is a typical character of Autler–Townes (AT) splitting [29]. The dip becomes more and more shallow, with the decrease of Δ/Γ characterizing the separation of the two resonances. The corresponding spectra with the maximum SGC ($\eta = 1$) are given in the right panels. Different from the case without SGC, one can always observe a dip with zero minimum in the total absorption. Once $\Delta/\Gamma < 1/2$ [Fig. 3(f)], we observe the following crucial changes: (i) the two resonances completely overlap (i.e., peak on peak); (ii) one resonance remains positive, indicating the absorption, whereas the other one becomes negative, indicating the gain; (iii) the positive resonance is wider than the negative one. Thus, the dip in total absorption can be regarded as an "imprint" of one resonance into the other, which is a result of a destructive

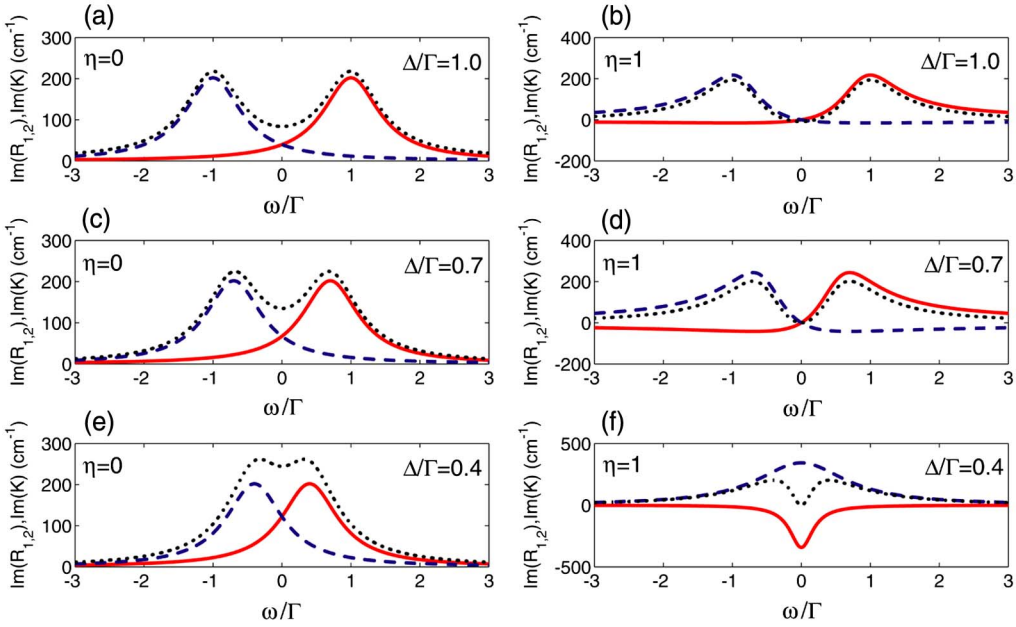

Fig. 3. (Color online) Im(R_1) (solid curve), Im(R_2) (dashed curve), and Im(K) (dotted curve) as functions of ω/Γ. (a), (c), (e) Spectra without SGC ($\eta = 0$) for $\Delta/\Gamma = 1.0$, 0.7, and 0.4, respectively. (b), (d), (f) Corresponding spectra with the maximum SGC ($\eta = 1$).

interference between the two resonances. In fact, this phenomenon comes from the quantum interference effect between two spontaneous emission channels (i.e., the spontaneous emission from $|2\rangle$ to $|1\rangle$ and that from $|3\rangle$ to $|1\rangle$), a typical character of SGC. From these results, we clearly see that it is the joint contribution from the AT splitting and the SGC effect that make the absorption of the probe field completely eliminated. Such a characteristic is very different from that of EIT systems, where linear absorption always exists. Thus, the SGC effect provides the possibility for an indeed long-distance transmission of the probe field in both the linear and nonlinear propagation regimes.

3. PULSE PROPAGATION IN NONLINEAR REGIME

Kerr nonlinearity is essential for most nonlinear optical processes, particularly for the formation of solitons. It can be largely enhanced in resonant optical media, but usually a serious optical absorption is accompanied simultaneously. Here, we show that in the present system, by the joint action of AT splitting and the SGC effect, the Kerr nonlinearity can be enhanced greatly without suffering optical absorption.

The probe-field susceptibility for the system is defined as

$$\chi_p = \frac{\mathcal{N}_a|\mathbf{e}_p\cdot\mathbf{d}_{12}|^2}{\epsilon_0\hbar}\frac{\rho_{21}+p\rho_{31}}{\Omega_p} \simeq \chi_p^{(1)}+\chi_p^{(3)}|\mathcal{E}_p|^2, \tag{10}$$

where $\chi_p^{(1)}$ and $\chi_p^{(3)}$ are linear and third-order susceptibilities, respectively. The real part of $\chi_p^{(3)}$ contributes to the Kerr nonlinearity, while the imaginary part of $\chi_p^{(3)}$ contributes to the nonlinear absorption or gain of the system. The explicit expressions of $\chi_p^{(1)}$ and $\chi_p^{(3)}$ can be obtained by solving Eq. (1) under the steady-state approximation, which reads

$$\chi_p^{(1)} = -\frac{\mathcal{N}_a|\mathbf{e}_p\cdot\mathbf{d}_{12}|^2}{\epsilon_0\hbar}\frac{p^2d_2+d_3-ip\eta\Gamma}{d_2d_3+\eta^2\Gamma^2/4}, \tag{11}$$

$$\chi_p^{(3)} = \frac{\mathcal{N}_a|\mathbf{e}_p\cdot\mathbf{d}_{12}|^4}{\epsilon_0\hbar^3}\frac{Ad_3+pBd_2-i(pA+B)\eta\Gamma/2}{d_2d_3+\eta^2\Gamma^2/4}. \tag{12}$$

The coefficients A and B in Eq. (12) are given by $A = r_{32}^* + 2r_{22} + r_{33}$ and $B = r_{32} + p(r_{22}+r_{33})$, where

$$r_{22} = \frac{-i\Gamma Y_1|d_{32}|^2 + X + \Gamma(Y_3d_{23}-Y_4d_{32})\zeta}{\Gamma^2|d_{32}|^2 + 2i\Gamma d_{23}\zeta^2 - 2i\Gamma d_{32}\zeta^2},$$

$$r_{33} = \frac{-i\Gamma Y_2|d_{32}|^2 - X + \Gamma(Y_3d_{23}-Y_4d_{32})\zeta}{\Gamma^2|d_{32}|^2 + 2i\Gamma d_{23}\zeta^2 - 2i\Gamma d_{32}\zeta^2},$$

$$r_{32} = \frac{2i(Y_3-Y_4)\zeta^2 - \Gamma Y_3d_{23} + (Y_1+Y_2)d_{23}\zeta}{\Gamma|d_{32}|^2 + 2id_{23}\zeta^2 - 2id_{32}\zeta^2}.$$

Here $X = (d_{23}-d_{32})(Y_1-Y_2)\zeta^2$, $Y_1 = -(d_3-ip\zeta)/(d_2d_3+\zeta^2) + (d_3^*+ip\zeta)/(d_2^*d_3^*+\zeta^2)$, $Y_2 = -(p^2d_2-ip\zeta)/(d_2d_3+\zeta^2) + (p^2d_2^*+ip\zeta)/(d_2^*d_3^*+\zeta^2)$, $Y_3 = -(pd_2-i\zeta)/(d_2d_3+\zeta^2) + (pd_3^*+ip^2\zeta)/(d_2^*d_3^*+\zeta^2)$, $Y_4 = -(pd_3-ip^2\zeta)/(d_2d_3+\zeta^2) + (pd_2^*+i\zeta)/(d_2^*d_3^*+\zeta^2)$, with $d_{32} = 2\Delta - i\Gamma$ and $\zeta = \eta\Gamma/2$.

Shown in Figs. 4(a) and 4(b) are $\mathrm{Re}(\chi^{(3)})$ and $\mathrm{Im}(\chi^{(3)})$ as functions of η, respectively. System parameters are taken as $\kappa = 1.0\times10^9\ \mathrm{cm^{-1}\,s^{-1}}$, $\Gamma = 1.0\times10^7\ \mathrm{s^{-1}}$, $\Delta = 5.5\times10^7\ \mathrm{s^{-1}}$, $\delta = 1.0\times10^7\ \mathrm{s^{-1}}$, and $p = 1$. From the figure we see that $|\mathrm{Re}(\chi^{(3)})|$ grows as η increases, whereas $|\mathrm{Im}(\chi^{(3)})|$ reduces as η increases. Thus, the SGC effect enhances the Kerr nonlinearity of the system significantly. In addition, $\mathrm{Re}(\chi^{(3)})$ has an order of $10^{-8}\ \mathrm{cm^{-1}\,s^2}$; i.e., it is 10^{12} times larger than that of conventional nonlinear optical media [30].

The Kerr nonlinearity enhancement obtained in the present atomic system can be used to balance the dispersion of the system and hence to obtain a nearly lossless and distortionless optical pulse propagation in the nonlinear regime. To this end, we apply the standard multiple-scale method to solve Eqs. (1) and (6), which is beyond the steady-state and adiabatic approximations [6,7]. We make the following asymptotic expansion $\rho_{jj} = \delta_{1j} + \sum_{n=1}^{\infty}\epsilon^n\rho_{jj}^{(n)}$ $(j = 1,\ 2,\ 3)$, $\rho_{ij} = \sum_{n=1}^{\infty}\epsilon^n\rho_{ij}^{(n)}$ $(i, j = 1, 2, 3,\ i \neq j)$, and $\Omega_p = \sum_{n=1}^{\infty}\epsilon^n\Omega_p^{(n)}$, where ϵ is a small parameter characterizing the small population depletion of the ground state. To obtain a divergence-free expansion, all quantities on the right-hand side of the expansion are considered as functions of the multiscale variables $z_l = \epsilon^l z$ $(l = 0, 1, 2)$ and $t_l = \epsilon^l t$ $(l = 0, 1)$. Substituting the expansion and the multiscale variables into Eqs. (1) and (6), we obtain a chain of linear, but inhomogeneous, equations that can be solved order by order.

At the leading order, we get the linear solution $\Omega_p^{(1)} = F\exp\{i[K(\omega)z_0 - \omega t_0]\}$ and the dispersion relation, given by Eq. (7). At the second order, a divergence-free condition requires $\partial F/\partial z_1 + (1/V_g)\partial F/\partial t_1 = 0$. Here F is a yet-to-be-determined envelope function depending on the slow variables t_1, z_1 and z_2. V_g is the group velocity.

The nonlinear equation for the envelope function F can be obtained at the third order; a divergence-free condition requires

$$i\frac{\partial F}{\partial z_2} - \frac{K_2}{2}\frac{\partial^2 F}{\partial t_1^2} - W\exp(-\bar{\beta}z_2)F|F|^2 = 0, \tag{13}$$

where $\bar{\beta} = \epsilon^{-2}\beta$ with $\beta = 2\mathrm{Im}(K_0)$ and

$$W = -\kappa\frac{Ad_3+pBd_2-i(pA+B)\eta\Gamma/2}{d_2d_3+\eta^2\Gamma^2/4},$$

with A and B being the same with those defined in Eq. (12).

After returning to original variables, Eq. (13) becomes

$$i\left(\frac{\partial}{\partial z}+\frac{\beta}{2}\right)U - \frac{K_2}{2}\frac{\partial^2 U}{\partial\tau^2} - W|U|^2U = 0, \tag{14}$$

where $\tau = t - z/V_g$ and $U = \epsilon F e^{-\bar{\beta}z_2/2}$. Equation (14) usually has complex coefficients due to the resonant character of the system. However, as we shall show below, under the joint

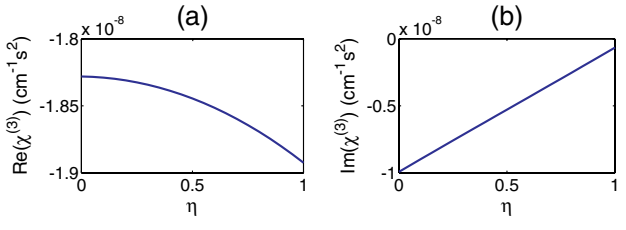

Fig. 4. (Color online) (a) $\mathrm{Re}(\chi^{(3)})$ and (b) $\mathrm{Im}(\chi^{(3)})$ as functions of η, respectively.

action of SGC and the AT splitting, a practical set of system parameters can be found to make the imaginary part of the coefficients be much smaller than their real part. Then Eq. (14) can be approximated as a nonlinear Schrödinger (NLS) equation, which allows soliton solutions being able to propagate for a rather long distance without significant attenuation and distortion. The dimensionless form of Eq. (14) is

$$i\frac{\partial u}{\partial s}+\frac{\partial^2 u}{\partial \sigma^2}+2u|u|^2=i\mu u, \tag{15}$$

where $s=-z/(2L_D)$, $\sigma=\tau/\tau_0$, and $u=U/U_0$, $\mu=2L_D/L_A$, with $L_D=\tau_0^2/|\tilde{K}_2|$ being the characteristic dispersion length, $L_A=1/\beta$ the characteristic absorption length, and $U_0=(1/\tau_0)\sqrt{|\tilde{K}_2/\tilde{W}|}$ the characteristic Rabi frequency of the probe field. The tilde symbol denotes the real part of the corresponding quantity.

If L_D is much less than L_A (i.e., $\mu \ll 1$, which is the case in the presence of SGC), the term on the right-hand side of Eq. (15) can be treated as a small perturbation and can be neglected at the first order. Hence, Eq. (15) reduces to the standard NLS equation, which is completely integrable and allows multisoliton solutions. After returning to the original variables, a single soliton solution of the NLS Eq. (15) corresponds to the half Rabi frequency of the probe field

$$\Omega_p=\frac{1}{\tau_0}\sqrt{\frac{\tilde{K}_2}{\tilde{W}}}\,\mathrm{sech}\left[\frac{1}{\tau_0}\left(t-\frac{z}{\tilde{V}_g}\right)\right]\exp\left[i\phi z-i\frac{z}{2L_D}\right]. \tag{16}$$

We now present a practical numerical example to support the above results. Consider a cold alkali atomic gas, for which the system parameters can be taken as $d_{24}\approx d_{34}=2.5\times10^{-27}$ cm^{-1} C, $\kappa=1.0\times10^9$ cm^{-1} s^{-1}, $\Gamma_2\approx\Gamma_3=1.0\times10^7$ s^{-1}, $\Delta=5.5\times10^7$ s^{-1}, $\delta=1.0\times10^7$ s^{-1}, and $p=1$. In Table 1 we list the values of K_0, K_1, K_2, and W without ($\eta=0$) and with ($\eta=1$) the maximum SGC. We note that SGC plays an important role to make the optical absorption of the system be largely eliminated; i.e., the imaginary part of K_0 is much smaller than its real part with the maximum SGC. However, the linear absorption characterized by the imaginary part of K_0 is not completely eliminated in this case. This is because we have set δ to be nonzero. If $\delta=0$, the coefficient W will be pure imaginary and hence no nonlinearity can be provided by the medium. In the absence of SGC, the value of the imaginary part of K_0 increases about 16 times, which means the appearance of a significant linear absorption and hence the probe field will attenuate rapidly. The propagating velocity of the soliton is given by

Table 1. K_0, K_1, K_2, and W without and with the Maximum SGC

	$\eta=0$	$\eta=1$
K_0(cm^{-1})	$6.66+i3.62$	$6.83+i0.23$
K_1(cm^{-1} s)	$(0.71+i0.07)\times10^{-6}$	$(0.73+i0.05)\times10^{-6}$
K_2(cm^{-1} s^2)	$(0.13+i0.09)\times10^{-13}$	$(0.14+i0.06)\times10^{-13}$
W(cm^{-1} s^2)	$(1.00+i0.05)\times10^{-14}$	$(1.00+i0.03)\times10^{-14}$

$$V_g=4.6\times10^{-5}c; \tag{17}$$

i.e., the soliton formed travels indeed with an ultraslow velocity. We must stress that the present scheme for generating the ultraslow optical soliton needs only one laser field, which is different from the EIT scheme, where at least two laser fields are required [5–7].

After taking $\tau_0=0.8\times10^{-7}$ s, we have $L_D=0.45$ cm, $U_0=1.5\times10^7$ s^{-1}, and $L_A=4.3$ cm with the maximum SGC. The generation power of the ultraslow optical soliton can be estimated by calculating the Poynting vector. The peak power $\tilde{P}_{\mathrm{peak}}\approx 2\epsilon_0 c n_p S_0(\hbar/|\mathbf{p}_{32}|)^2U_0^2$, with n_p and S_0 being the reflective index and the cross-section area of the probe beam, respectively. With the above parameters, it is easy to estimate

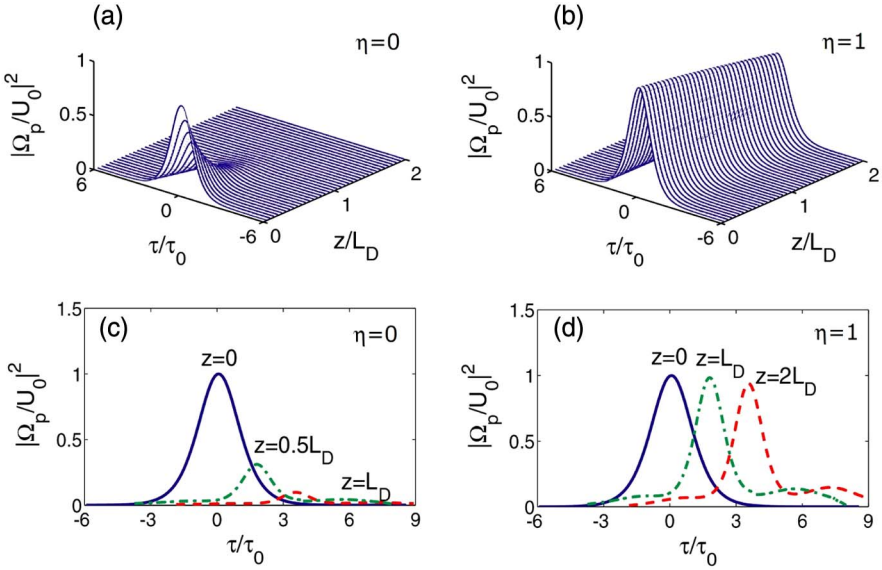

Fig. 5. (Color online) (a), (b) Wave shapes of $|\Omega_p/U_0|^2$ as a function of z/L_D and τ/τ_0 with (a) $\eta=0$ and (b) $\eta=1$]. The results are numerically obtained from Eq. (14) with full complex coefficients taken into account. (c), (d) Wave shapes of $|\Omega_p/U_0|^2$ as a function of τ/τ_0 with (c) $\eta=0$ and (d) $\eta=1$. The results are obtained by directly integrating Eqs. (1) and (6) at $z=0$, $0.5L_{\mathrm{Diff}}$, and L_{Diff} in (c) and at $z=0$, L_{Diff}, and $2L_{\mathrm{Diff}}$ in (d).

the peak power of the ultraslow optical soliton, which is given as

$$\bar{P}_{\text{peak}} = 0.65\ \mu\text{W}, \tag{18}$$

with $S_0 = \pi \times 10^{-4}$ cm^2. Thus, we see that very low power is needed for generating the ultraslow optical soliton due to the enhancement of Kerr nonlinearity.

We have also studied the propagation of the ultraslow optical soliton presented above by using numerical simulations. Shown in Figs. 5(a) and 5(b) are the wave shapes of $|\Omega_p/U_0|^2$ as a function of z/L_D and τ/τ_0 without ($\eta = 0$) and with ($\eta = 1$) the maximum SGC, respectively. We see that the soliton is completely absorbed in a short propagation distance without SGC. However, its amplitude undergoes only a slight decrease while its width undergoes a slight increase after propagating a long distance with the maximum SGC.

Finally, we have made a numerical simulation by directly integrating Eqs. (1) and (6) to confirm the analytical prediction. The results are shown in Figs. 5(c) and 5(d). We see that, contrary to the case without SGC, the solitons obtained with the maximum SGC can indeed propagate a long distance without significant attenuation.

4. DISCUSSION AND SUMMARY

SGC occurs in systems having near-degenerated levels with the same angular momentum quantum numbers J and m_J and nonorthogonal dipole moments, which are usually hard to satisfy in atomic media [31]. However, in a recent experiment [32], SGC has been observed in a rubidium atoms with N- and inverted Y-type level configurations. In addition, the quantum interference via SGC can be observed in many other systems such as semiconductor quantum wells and quantum dots [33–35], autoionizing media [36], and the anisotropic vacuum [37]. Our theoretical approach presented above can be easily generalized to these systems with SGC.

We have also considered other two types of three-state quantum system, i.e., the Λ- and Ξ-type systems with SGC [13,38,39]. However, calculating results (which are omitted here) show that SGC has no effect on the dispersion and absorption and no Kerr-nonlinearity enhancement can be obtained. Hence the Λ- and Ξ-type systems with SGC cannot be taken to realize a nearly lossless propagation of ultraslow optical solitons.

In conclusion, in this work we have proposed a new scheme to generate stable ultraslow optical solitons in lifetime-broadened three-state V-type media through SGC). We have shown that in the linear propagation regime, SGC in the system can result in a significant change of dispersion and absorption and may be used to completely eliminate the absorption and greatly reduce the group velocity of probe field. In the nonlinear propagation regime, SGC can largely enhance the Kerr nonlinearity of the system. We demonstrated that by means of SGC, stable optical solitons with ultraslow propagating velocity and ultralow generation power can be produced. Different from previous works via EIT, ultraslow optical solitons obtained in the present system based on the atomic coherence via SGC have much smaller attenuation during propagation and can be created by using only one laser field.

ACKNOWLEDGMENTS

This work was supported by the National Natural Science Foundation of China under grant nos. 10874043, 11174080, and 11105052 and by the Open Fund from the State Key Laboratory of Precision Spectroscopy, ECNU.

REFERENCES AND NOTES

1. S. L. McCall and E. L. Hahn, "Self-induced transparency by pulsed coherent light," Phys. Rev. Lett. **18**, 908–911 (1967).
2. M. J. Konopnicki and J. H. Eberly, "Simultaneous propagation of short different-wavelength optical pulses," Phys. Rev. A **24**, 2567–2583 (1981).
3. R. Grobe, F. T. Hioe, and J. H. Eberly, "Formation of shape-preserving pulses in a nonlinear adiabatically integrable system," Phys. Rev. Lett. **73**, 3183–3186 (1994).
4. M. Fleischhauer, A. Imamoglu, and J. P. Marangos, "Electromagnetically induced transparency: optics in coherent media," Rev. Mod. Phys. **77**, 633–673 (2005), and references therein.
5. Y. Wu and L. Deng, "Ultraslow optical solitons in a cold four-state medium," Phys. Rev. Lett. **93**, 143904 (2004).
6. G. Huang, L. Deng, and M. G. Payne, "Dynamics of ultraslow optical solitons in a cold three-state atomic system," Phys. Rev. E **72**, 016617 (2005).
7. C. Hang, G. Huang, and L. Deng, "Generalized nonlinear Schrödinger equation and ultraslow optical solitons in a cold four-state atomic system," Phys. Rev. E **73**, 036607 (2006).
8. G. S. Agarwal, *Quantum Optics*, Springer Tracts in Modern Physics, Vol. **70** (Springer, 1974).
9. S. E. Harris, "Lasers without inversion: interference of lifetime-broadened resonances," Phys. Rev. Lett. **62**, 1033–1036 (1989).
10. A. Imamoğlu, "Interference of radiatively broadened resonances," Phys. Rev. A **40**, 2835–2838 (1989).
11. J. H. Wu and J. Y. Gao, "Phase control of light amplification without inversion in a Λ system with spontaneously generated coherence," Phys. Rev. A **65**, 063807 (2002).
12. Y. Bai, H. Guo, H. Sun, D. Han, C. Liu, and X. Chen, "Effects of spontaneously generated coherence on the conditions for exhibiting lasing without inversion in a V system," Phys. Rev. A **69**, 043814 (2004).
13. S. Menon and G. S. Agarwal, "Effects of spontaneously generated coherence on the pump-probe response of a Λ system," Phys. Rev. A **57**, 4014–4018 (1998).
14. S. Y. Zhu, R. C. F. Chan, and C. P. Lee, "Spontaneous emission from a three-level atom," Phys. Rev. A **52**, 710–716 (1995).
15. S. Y. Zhu and M. O. Scully, "Spectral line elimination and spontaneous emission cancellation via quantum interference," Phys. Rev. Lett. **76**, 388–391 (1996).
16. P. Zhou and S. Swain, "Ultranarrow spectral lines via quantum interference," Phys. Rev. Lett. **77**, 3995–3998 (1996).
17. E. Paspalakis and P. L. Knight, "Phase control of spontaneous emission," Phys. Rev. Lett. **81**, 293–296 (1998).
18. K. T. Kapale, M. O. Scully, S. Y. Zhu, and M. S. Zubairy, "Quenching of spontaneous emission through interference of incoherent pump processes," Phys. Rev. A **67**, 023804 (2003).
19. I. Gonzalo, M. A. Antón, F. Carreño, and O. G. Calderón, "Squeezing in a Λ-type three-level atom via spontaneously generated coherence," Phys. Rev. A **72**, 033809 (2005).
20. Y. P. Niu and S. Q. Gong, "Enhancing Kerr nonlinearity via spontaneously generated coherence," Phys. Rev. A **73**, 053811 (2006).
21. D. G. Norris, L. A. Orozco, P. Barberis-Blostein, and H. J. Carmichael, "Observation of ground-state quantum beats in atomic spontaneous emission," Phys. Rev. Lett. **105**, 123602 (2010).
22. Z. Tang, G. Li, and Z. Ficek, "Entanglement created by spontaneously generated coherence," Phys. Rev. A **82**, 063837 (2010).
23. R. G. Wan, J. Kou, L. Jiang, Y. Jiang, and J. Y. Gao, "Electromagnetically induced grating via enhanced nonlinear modulation by spontaneously generated coherence," Phys. Rev. A **83**, 033824 (2011).
24. E. Paspalakis, N. J. Kylstra, and P. L. Knight, "Transparency induced via decay interference," Phys. Rev. Lett. **82**, 2079–2082 (1999).

25. D. A. Cardimona, M. G. Raymer, and C. R. Stroud, Jr., "Steady-state quantum interference in resonance fluorescence," J. Phys. B **15**, 55–64 (1982).
26. The frequency and wavenumber of the probe field are given by $\omega_p + \omega$ and $k_p + K(\omega)$, respectively. Thus, $\omega = 0$ corresponds to the center frequency of the probe field.
27. P. M. Anisimov and O. Kocharovskaya, "Decaying-dressed-state analysis of a coherently driven three-level Λ system," J. Mod. Opt. **55**, 3159–3171 (2008).
28. P. M. Anisimov, J. P. Dowling, and B. C. Sanders, "Objectively discerning Autler–Townes splitting from electromagnetically induced transparency," Phys. Rev. Lett. **107**, 163604 (2011).
29. T. Y. Abi-Salloum, "Electromagnetically induced transparency and Autler–Townes splitting: two similar but distinct phenomena in two categories of three-level atomic systems," Phys. Rev. A **81**, 053836 (2010).
30. S. Saltiel, S. Tanev, and A. D. Boardman, "High-order nonlinear phase shift caused by cascaded third-order processes," Opt. Lett. **22**, 148–150 (1997).
31. H. R. Xia, C. Y. Ye, and S. Y. Zhu, "Experimental observation of spontaneous emission cancellation," Phys. Rev. Lett. **77**, 1032–1034 (1996).
32. S.-C. Tian, Z.-H. Kang, C.-L. Wang, R.-G. Wan, J. Kou, H. Zhang, Y. Jiang, H.-N. Cui, and J.-Y. Gao, "Observation of spontaneously generated coherence on absorption in rubidium atomic beam," Opt. Commun. **285**, 294–299 (2012).
33. J. Faist, F. Capasso, C. Sirtori, K. W. West, and L. N. Pfeiffer, "Controlling the sign of quantum interference by tunnelling from quantum wells," Nature **390**, 589–591 (1997).
34. H. Schmidt, K. L. Campman, A. C. Gossard, and A. Imamoğlu, "Tunneling induced transparency: Fano interference in intersubband transitions," Appl. Phys. Lett. **70**, 3455–3457 (1997).
35. J. H. Wu, J. Y. Gao, J. H. Xu, L. Silvestri, M. Artoni, G. C. La Rocca, and F. Bassani, "Ultrafast all optical switching via tunable Fano interference," Phys. Rev. Lett. **95**, 057401 (2005).
36. T. Nakajima, "Linear and nonlinear optical properties of an autoionizing medium," Phys. Rev. A **63**, 043804 (2000).
37. G. S. Agarwal, "Anisotropic vacuum-induced interference in decay channels," Phys. Rev. Lett. **84**, 5500–5503 (2000).
38. J. Javanainen, "Effect of state superpositions created by spontaneous emission on laser-driven transitions," Europhys. Lett. **17**, 407–412 (1992).
39. Z. Ficek, B. J. Dalton, and P. L. Knight, "Fluorescence intensity and squeezing in a driven three-level atom: ladder case," Phys. Rev. A **51**, 4062–4077 (1995).